Removal of Ni(II), Zn(II) and Pb(II) from aqueous solutions using cation-exchange resin in fixed-bed column

Myzairah Hamdzah[a], Zaini Ujang[b], Mohamed Mahmoud Nasef[c,*], Norhayati Abdullah[d], Farrah Aini Dahalan[e]

[a]*Centre for Innovative Planning & Development (CIPD), Research Institute of Sustainable Environment (RISE), UTM, 81310 Johor Bahru, Johor, Malaysia, Tel. +607 5557340; email: myzairah@gmail.com*
[b]*Ministry of Education, Presint 5, 62200 Putrajaya, Malaysia, Tel. +603 88705051; email: zainiujang@moe.gov.my*
[c]*Center for Hydrogen Energy, Institute of Future Energy, Universiti Teknologi Malaysia, Jalan Semarak, 54000 Kuala Lumpur, Malaysia, Tel. +603 22031229; email: mahmoudeithar@cheme.utm.my*
[d]*UTM Palm Oil Research Center, Block T02, UTM, 81310 Johor Bahru, Johor, Malaysia, Tel. +607 5557534; email: norhayatiabdullah@fbb.utm.my*
[e]*The School of Environmental Engineering, Universiti Malaysia Perlis, Kompleks Pengajian Kejuruteraan Jejawi 3, 02600 Arau, Perlis, Malaysia, Tel. +604 9798985; email: farrahunimap@gmail.com*

Received 1 July 2014; Accepted 8 September 2015

ABSTRACT

Breakthrough curves for the removal of Ni(II), Zn(II), and Pb(II) from aqueous solutions using cation exchange resin (Dowex 50W) were determined at dynamic conditions in a fixed-bed column under ambient temperature. The experiments and data obtained were designed and analyzed using response surface methodology, respectively. Three operating parameters: flow rate (15–25 mL min^{-1}), pH (3–9), and bed height (3–5 cm) were investigated. Fixed-bed adsorption models namely Thomas model and Bohart–Adam model were adopted to describe the dynamics of metal adsorption in the column. The obtained experimental data were fitted to these models based on the kinetic constant k_{BA} (mg min cm^{-3}), k_{TH} (cm^3 mg^{-1} min), the maximum amount of metal exchange N_0 (mg cm^{-3}), and the maximum adsorption capacities $q_t m$ (mg), accordingly. The Thomas model was found to best fit all the experimental conditions studied with correlation coefficients of 0.91, 0.97, and 0.92 for Ni(II), Zn(II), and Pb(II), respectively.

Keywords: Cation exchange resins; Heavy metal; Bohart–Adam model; Thomas model

1. Introduction

The increasing amount of metals and chemicals used in various industrial processes, such as metal plating, mining, fertilizer production, tanning, battery manufacturing, and paper making have generated large volume of effluents containing high levels of heavy metals. These contaminated effluents cause environmental problems in terms of their disposal owing to their non-biodegradability and tendency to accumulate in living organisms [1]. Furthermore, the leaking of heavy metals into the soil can lead to groundwater and surface water contamination. Consequently, these can adversely affect human, animal, and aquatic lives.

*Corresponding author.

Wastewater from the battery industries contains large amount of heavy metals, such as Cd(II), Hg(II), Cu(II), Pb(II), Ni(II), and Zn(II), that must be treated prior to safe disposal into the environment. According to the Malaysian-Environmental Quality Act 1974 (Sewage and Industrial Effluents) [2], the maximum discharge limits for Ni(II) and Zn(II) under standard B is 1.0 mg L^{-1}, while Pb(II) amount is limited to 0.5 mg L^{-1}. A number of researchers studied the removal of various types of metal ions from aqueous solution using natural, synthetic, and chelating ion exchange [3–12]. It was discovered that the removal of metal ions using ion-exchange resins has high potential for industrial wastewater treatment. Among heavy metals, Pb(II), Zn(II), and Ni(II) are of particular interest because of their toxicity and widespread presence in many of industrial applications.

The ion exchange is an effective technique for the removal of heavy metal ions from water and wastewater [13]. The possibility of ion exchange or chelating process to remove heavy metals ion from aqueous solution has been explored extensively [14–16]. The removal of lead, zinc, and nickel in batch column was successfully demonstrated by Pehlivan and Altun [13]. The maximum sorption of strontium from aqueous solution was successfully determined by Hafizi et al. [17] using Dowex 50W. Previous studies reported that Dowex 50W was several times more efficient than the conventional resins and other natural adsorbents in removing toxic and harmful transition metal ions from aqueous solutions. Dowex resins are robust, insoluble, and compatible with various treatment conditions. Resins in the form of sodium impart both stability and long shelf life: hence, it can withstand longer period in high concentration heavy metals absorption [13]. In addition, their operation cost is shown to be cheaper as compared to other synthetic resins [18].

Selection of the most appropriate resin for a particular situation requires a careful balance of physical and chemical properties of the resins as well as of the solution, in which to be treated significantly [13,18]. Two main ion-exchange systems: batch continuous stirred reactor and fixed-bed column reactor are available for evaluating effective resin utilization. Batch system is used to provide a simpler method for establishing the effects of various experimental parameters, such as pH, temperature, and initial concentration on the removal efficiency. It is also used to determine the optimum amount of resins needed for a column mode operation or to determine the kinetics of a certain resin [19]. However, batch column experiments were less convenient to use on industrial scale, where large volumes of wastewater are continuously generated. In order to understand the characteristic behavior of

resin (DOWEX) in a real heavy metal sorption, the study conducted in continuous sorption system is required. Therefore, in this work, a number of experiments were conducted using continuously fixed-bed column reactor. This study focuses on establishing the shape of breakthrough curve and its velocity through the fixed-bed system. An experimental design with response surface analysis is used to evaluate the significance of operating parameters, such as the flow rate, pH, and bed height (BH) on the column performance. This statistical approach allows systematic and more appropriate variation of the experimental conditions in a way leading to reduce the number of experiments, optimize treatment conditions, and to demonstrate/propose/project the model of the system performance. The breakthrough curves for the adsorption of three types of metal ions were analyzed using Bohart–Adam and Thomas models. Further, modeling on the adsorption dynamics of the fixed bed was presented, and finally the correlation between the model and the experimental data was established.

2. Experimental

2.1. Materials

Dowex 50W was obtained from Fluka Co (St. Loius, MO, USA). The properties of the resins are presented in Table 1. Prior to use, the resin was washed with deionized water and then dried in a vacuum oven at 50°C overnight. A known quantity of (Zn(NO$_3$)$_2$·6H$_2$O) from ChemPur (Karlsruhe, Germany) (M_w = 297.47 g mol^{-1}), lead ions, lead(II) nitrate from HmbG (M_w = 331.20 g mol^{-1}), and nickel ions, nickel(II) nitrate (Ni(NO$_3$)$_2$·6H$_2$O) from QRec (M_w = 290.81 g mol^{-1}) were weighed before adding to the deionized water. All chemicals and reagents used were of analytical grade. Solutions of 0.1 M NaOH and 0.1 M HNO$_3$ were used for pH adjustment, respectively.

2.2. Fixed-bed adsorption studies

Breakthrough curves experiments were planned using a response surface design at different operating parameters, such as feed flow rate (Q, mL min^{-1}), pH, and bed height (cm). Each factor was changed to different levels according to the experimental design given in Table 2, resulting in a total of 20 experiments.

These experiments were carried out at room temperature (27°C) in a clear perspex column with an internal diameter of 2 cm and length of 20 cm. The up-flow ion-exchange column was fed by a peristaltic pump. The samples in the outlet were taken at

Table 1
Properties of Dowex 50W

Type	Strong acid cation exchanger Dowex 50W-X8
Active group	Sulfonic acid
Matrix	Gel(microporous)-styrene divinylbenzene
Ionic forms as shipped	H^+
Physical form	Spherical beads
Standard mesh sizes (wet)	20–50
Mean particle size (μm)	560
Effective pH range	0–14
Total exchange capacity	H^+ form
meq g^{-1} dry resin	4.8

predetermined time intervals until the resin reached saturation point; the saturation was monitored by analyzing the concentration of each ion in the collected samples. A new batch of cationic resin was used in each experimental run. According to the literature, the effects of near-wall disturbances and preferential channels in the column were neglected if the ratio of the internal column diameter to the resin particle diameter is higher than 10 (approximately 14.5) [20].

2.3. Breakthrough analysis

The time and shape of the breakthrough appearance are very important characteristics for determining the operation and the dynamic response of fixed-bed column. Therefore, breakthrough curves (C/C_o vs. time) were plotted, where C is the effluent concentration (mg L^{-1}), and C_o is the inlet metal ion solutions (mg L^{-1}). The breakthrough time (t_{br}) and saturation time (t_{end}) also were used to evaluate the breakthrough curve. The efficiency of solute removal, ε_r, and the efficiency of resin utilization, ε_f, defined by Eqs. (1) and (2), respectively. A statistical analysis of the results was developed using these values to allow the evaluation of the process performance.

$$\varepsilon_r = \frac{QC_o\left(t_{br} - \int_0^{t_{br}}\left(\frac{C}{C_o}\right)dt\right)}{QC_o t_{br}} \tag{1}$$

$$\varepsilon_f = \frac{QC_o\left(t_{br} - \int_0^{t_{br}}\left(\frac{C}{C_o}\right)dt\right)}{QC_o\left(t_{end} - \int_0^{t_{end}}\left(\frac{C}{C_o}\right)dt\right)} \tag{2}$$

where Q is the volumetric flow rate (mL min^{-1}). The following response function (RF), (Eq. (3)) is suggested in order to use the experimental breakthrough curves for process optimization. This RF takes into account both efficiencies. The formulation also considers the

breakthrough time. In process productivity, it is important that the time period for maximum solute removal is minimized. This RF seems to be the optimal term to represent the process performance because it combines both resin utilization and solute removal (i.e. the period before breakthrough time).

$$\text{Response function (RF)} = \frac{\varepsilon_r \varepsilon_f}{t_{br}} \tag{3}$$

2.4. Bohart–Adams model

Prediction of the breakthrough curve and exchange capacity under specific operating conditions is required for the design of a column exchange process. The Bohart–Adams model assumes/considers that the adsorption rate is proportional to both the residual capacity of the resins and the concentration of the sorbing species as represented by the following equation:

$$\ln\left(\frac{C_o}{C} - 1\right) = \frac{K_{BA}N_o Z}{U_o} - K_{BA}C_o t \tag{4}$$

where C is the effluent concentration (mg cm^{-3}), C_o is the influent concentration (mg cm^{-3}), K_{BA} is the rate coefficient (cm^3 mg^{-1} min^{-1}), N_o is the exchange capacity (mg cm^{-3}), Z is the BH (cm), U_o is the linear velocity (cm min^{-1}), and t is the time (min). The model constants K_{BA} and N_o can be determined from a plot of $\ln[(C/C_o) - 1]$ against t (Fig. 4(a)) for a given flow rate and BH. The details of Bohart–Adams Model can be found elsewhere [21,22].

2.5. Thomas model

Thomas model, which describes the relation between the adsorption capacity and feed concentration, is expressed by the following equation:

Table 2
Efficiency for the experimental breakthrough curves

Flow rate (mL min⁻¹) (±0.5)	pH (±0.5)	Bed height (cm)	Ni(II)					Zn(II)					Pb(II)				
			T_{br} (min) (±2)	T_{end} (min) (±2)	ε_r	ε_f	RF	T_{br} (min) (±2)	T_{end} (min) (±2)	ε_r	ε_f	RF	T_{br} (min) (±2)	T_{end} (min) (±2)	ε_r	ε_f	RF
15.2	4.2	2.8	90	240	0.98	0.50	0.005	120	270	0.99	0.40	0.003	270	420	0.99	0.88	0.003
24.8	4.2	2.8	60	210	0.99	0.47	0.008	100	210	0.96	0.38	0.003	210	360	0.99	0.70	0.003
15.2	7.8	2.8	90	300	0.99	0.50	0.006	150	240	0.99	0.44	0.003	180	390	0.98	0.68	0.004
24.8	7.8	2.8	60	240	0.99	0.47	0.008	100	210	0.99	0.70	0.007	210	390	0.99	0.78	0.004
15.2	4.2	5.2	120	270	0.99	0.72	0.006	120	360	0.99	0.79	0.006	150	420	0.99	0.97	0.006
24.8	4.2	5.2	90	240	0.97	0.75	0.008	100	330	0.98	0.53	0.005	210	240	0.99	0.71	0.003
15.2	7.8	5.2	120	300	0.99	0.73	0.006	120	420	0.99	0.66	0.005	120	390	0.99	0.54	0.004
24.8	7.8	5.2	90	270	0.99	0.73	0.008	120	390	0.99	0.58	0.004	180	300	0.99	0.74	0.004
12.0	6.0	4.0	150	240	0.99	0.77	0.005	210	420	1.00	0.73	0.003	150	360	0.96	0.61	0.004
28.0	6.0	4.0	30	150	0.93	0.36	0.011	150	270	0.99	0.84	0.005	240	270	0.99	0.81	0.003
20.0	3.0	4.0	60	240	0.96	0.42	0.007	300	420	0.99	0.92	0.003	210	420	0.97	0.81	0.004
20.0	9.0	4.0	60	240	0.96	0.42	0.007	180	420	0.99	0.70	0.003	180	390	0.99	0.74	0.004
20.0	6.0	2.0	60	150	0.87	0.40	0.006	150	330	0.99	0.56	0.003	180	390	0.99	0.75	0.004
20.0	6.0	6.0	120	270	0.99	0.92	0.008	180	420	0.99	0.74	0.004	180	390	0.99	0.78	0.004
20.0	6.0	4.0	60	240	0.99	0.40	0.007	90	270	0.99	0.33	0.003	240	390	0.99	0.79	0.003
20.0	6.0	4.0	60	240	0.99	0.40	0.007	120	270	0.99	0.38	0.003	240	390	0.98	0.78	0.003
20.0	6.0	4.0	90	270	0.99	0.61	0.007	120	270	0.98	0.38	0.003	210	390	0.99	0.80	0.004
20.0	6.0	4.0	60	240	0.96	0.43	0.007	150	300	0.99	0.47	0.003	150	390	0.99	0.63	0.004
20.0	6.0	4.0	60	240	0.96	0.43	0.007	150	240	0.99	0.44	0.002	210	390	0.99	0.80	0.004
20.0	6.0	4.0	90	270	0.97	0.62	0.006	90	240	0.98	0.29	0.003	240	390	0.98	0.79	0.003

$$\ln\left(\frac{C_o}{C} - 1\right) = \frac{K_{TH}q_T m}{Q} - K_{TH}C_o t \qquad (5)$$

where K_{TH} is the rate coefficient (cm^3 mg^{-1} min^{-1}), $q_T m$ is the maximum adsorption capacity with total mass of the adsorbent (mg). The model constants K_{TH} and $q_T m$ can be determined from a plot of $\ln[(C_o/C) - 1]$ against t for a given flow rate [22].

3. Results and discussion

3.1. Breakthrough curves for heavy metal removal

3.1.1. Effect of flow rate

The column studies were carried out at five different flow rates (11.6, 15.0, 20.0, 25.0, and 28.4 mL min^{-1}). The efficiencies were calculated according to Eqs. (2) and (3) and the corresponding experimental conditions are given in Table 2. The highest value of resin utilization is 0.77 at a flow rate of 12 mL min^{-1}, saturation time 240 min, and the lowest value is 0.36 at flow rate 28 mL min^{-1}, saturation time 150 min at the same BH (4 cm). As expected, the results indicate that for higher flow rates, the breakthrough time (t_{br}) and saturation time (t_{end}) occur sooner due to the resin property. The efficiency of resin utilization for metal ions removal increases as the flow rate decreases. This behavior can be explained in terms of the residence time of the metal in the column in which the increase in the flow rate reduces the volume treated efficiently until the breakthrough point. This is because of the insufficient contact time between the metal ions and the cation exchange resin (Dowex 50W), which limits the number of available sites, thus reducing the volume of metal ions solution to be treated. In addition, high flow rate could lead to the detachment of the weak ionic bonds between the metal ions and the binding sites of the resins. Similar remarks were made upon experimental investigation of breakthrough curves for the uptake of oleic acid from azeotropic ethanol solutions using Amberlyst-26A anion exchange resin as a function of operational conditions using response surface methodology [23]. It was reported that when the flow rate decreases, the contact time or the time for mass transfer in the column gets longer, and the resin utilization becomes more effective [20,24]. Hence, the metal ions could have better affinity to diffuse to the active sites within the cation exchange resins, which were not easily reached under normal condition. This could lead to the better sorption efficiency and increased the saturation time of the system [6].

3.1.2. Effect of BH

One of other factors that have great effect on metal ions removal efficiency in a fixed-bed column is the height of resins in the column. Table 2 shows that the breakthrough volume varies with different BH (2.0, 2.8., 4.0, 5.2, and 6.0 cm). The highest value of resin utilization is 0.92 at BH 6 cm, and 0.42 at BH 2 cm at the same flow rate. This trend can be attributed to the nature of mass transfer phenomena taking place during the process. In particular, the reduction in BH leads to predominance of mass transfer by an axial dispersion phenomenon, which in turn reduces the diffusion of metal ions. Thus, the metal ions do not have sufficient time to diffuse into the whole sector of the packed resin bed. This trend is going a long with adsorption time for lead(II) on *Pinus sylvestris* sawdust and adsorption of Cd(II) on coir pith column in a continuous flow removal [25,26].

Response surface 3D plots representing the relationship between efficiency of solute removal, pH value, and BH are shown in Fig. 1. It shows that the efficiency of solute removal increases with increase in the BH for the types of metal ions. As the height of the bed increases, the time required to reach breakthrough and saturation phase increases significantly. This was reported to be due to the availability of increasing number of sorption sites [27]. The mass of the cation exchange resin is proportional to the BH, thus, a higher BH lead to a larger exchange capacity and higher efficiency of solute removal. This behavior is shown in Fig. 2 for all three types of the metals studied. In this figure, response surface 3D plots representing relationship between efficiency of resin utilization, flow rate, and BH. This means that the volume of aqueous solution that can be treated was effectively increased. Similar behavior was reported for dynamic removal of copper by Na-form of Purolite C100-MB cation exchange resin in packed bed columns under batch conditions with varying BHs and flow rates [20].

In Fig. 2, there are different trends shown for each metal ions. The average trend was viewed for resin utilization for Pb(II) removal. This may be due to the effect of ion selectivity. From this figure, it can be concluded that the resins are most utilized for Pb(II) removal for each level of operating parameters. For Ni(II), the efficiency of resin utilization increased with the increase BH. At a lower flow rate, higher BH increased the efficiency of resin utilization for Zn(II) removal. Similar explanation is due to the availability of an increasing number of sorption sites and contact time.
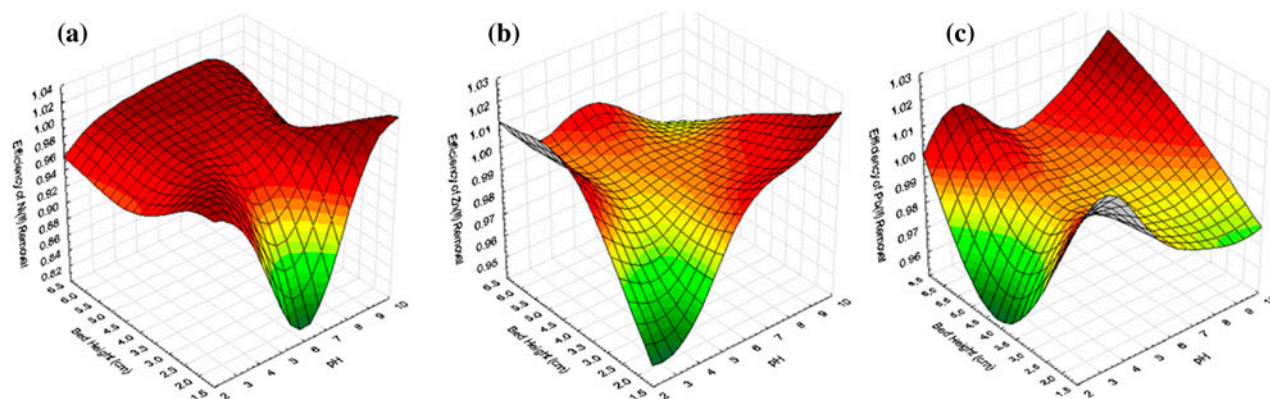
Fig. 1. Response surface 3D plot representing the relationship between efficiency of metal removal, BH (cm), and the pH value: (a) Ni(II), (b) Zn(II), and (c) Pb(II).
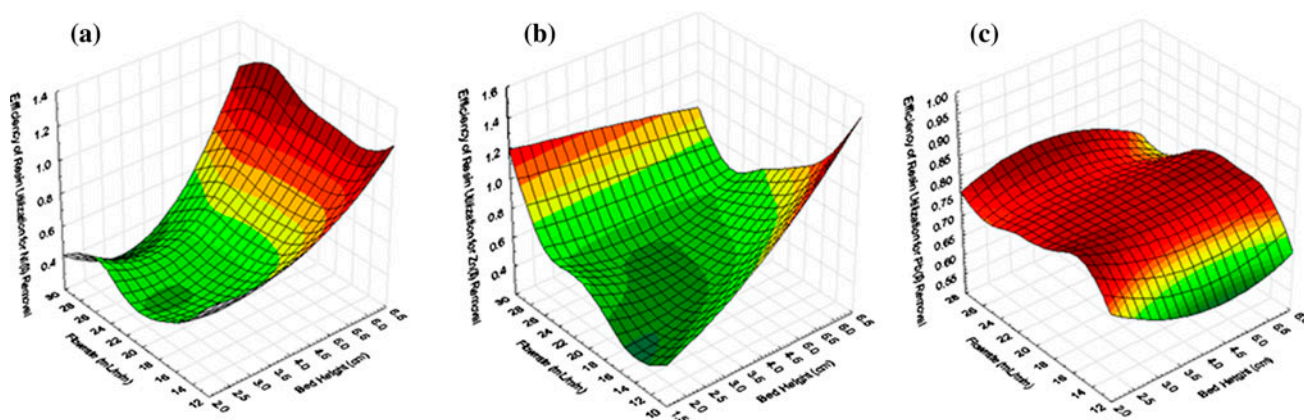

Fig. 2. Response surface 3D plot representing the relationship between efficiency of resin utilization, flow rate (mL min^{-1}), and the pH value: (a) Ni(II), (b) Zn(II), and (c) Pb(II).

3.1.3. Effect of pH

The value of pH is one of the important parameter influencing the exchange capacity. The initial solution pH could influence the mechanism of ion-exchange process in terms of metal ions adsorption which is known as selectivity. The explanation and interactions of these metals with Dowex 50W resins are complex. This is most likely due to simultaneous processes of both adsorption and ion exchange. Dowex 50W is a sulfonic acid group resin, which is able to function well at all pH ranges [13]. Therefore, the investigation of the effect of pH was performed in the range 3.0–9.0. Fig. 1 shows that the efficiency of Zn(II) removal increased with increasing the pH value, and the lowest efficiency is at pH 2. The lowest value of adsorption capacity for Ni(II), Zn(II), and Pb(II) at lower pH conditions are 0.88,

0.76, and 1.02 meq g^{-1} of dry resin, respectively. The efficiency of both metals (Ni(II) and Pb(II)) removal was increased before and after pH 6.5 at lower BH. However, the efficiency of all metal removal is higher (Ni(II) (0.96–1.00); Zn(II) (0.98–1.01); Pb(II) (0.99–1.02)) with increasing the BH at all pH ranges. The value of efficiencies for metal removals show the selectivity increases in the series: Pb(II) > Zn(II) > Ni(II). The average amount of sorbed metal ion per gram dry resin was calculated as 1.43, 2.94, and 2.95 meq g^{-1} dry resin for Ni(II), Zn(II), and Pb(II), respectively. However, the ion-exchange capacity for Dowex 50W resins was reported to be 4.8 meq g^{-1} dry resin as compared to the adsorption capacities for the experimental Ni(II), Zn(II), and Pb(II). The presence of other metal ions may have contributed to the lower adsorption capacity besides the concur-

rent effects of charge valence, increasing atomic number, and degree of ionization of the exchanged metal [28].

As for metal ions species, the degree of its adsorption onto the adsorbent surface is influenced by the ionic charge on the surface of the adsorbent. This sorption trend can be described as the effect of competitive binding between three types of metals and hydrogen ions for the binding sites on the surface of the resins. The competition between both active adsorption sites has resulted in a lower efficiency of solute removal at pH 6.5. As the pH increases, the adsorption zones tend to attain less positive charges, leading to an increase in electrostatic attraction between the metal ions and sulfonic acid groups. The adsorption capacity increases with the decreasing of radius size of hydrated metal ions. These findings are in good agreement with literatures [29–31].

3.2. Response surface analysis

The formulation of RF considered the efficiencies of solute removal, resin utilizations, and breakthrough time. This RF seems to be suitable for representing the process performance because it combines both efficiencies and the required time interval in terms of metal ions removal. The statistical analysis generated the formulated model as presented in Eq. (6), which describes the RF in terms of two operating parameters i.e. flow rate (mL min^{-1}) and BH (cm). It shows that lower efficiency of resin utilization (ε_f) can be compensated by decreasing the breakthrough time (t_{br}). The increase in the flow rate
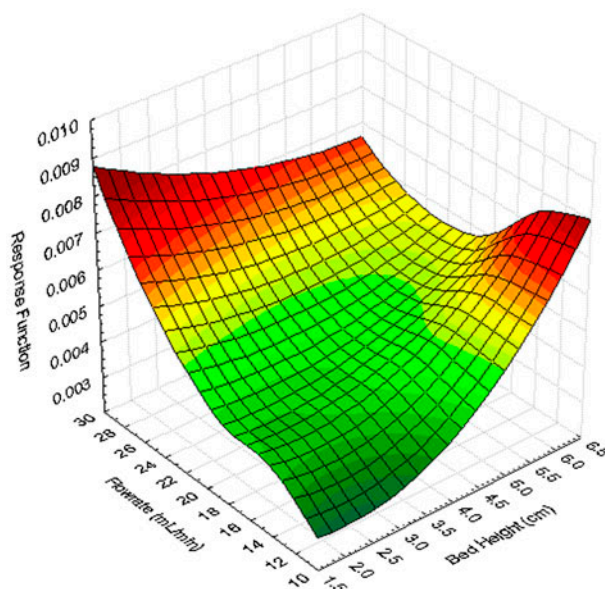

Fig. 3. Response surface 3D plot representing the relationship between RF (average value for three metal ions), flow rate (mL min^{-1}) and BH (cm).

led to a decrease in the efficiency of resin utilization. This is due to the lower residence time of the solution in the resin bed.

This formulated model supports the explanation for the RF in terms of the investigated parameters with a significance level of 99%. Based on summary of the p-value in Table 3, the R^2 value of the model is acceptable (91.4%) and the p-value of the lack-of-fit (0.241) indicates it was significant, which implies that the predictive knowledge of the model was statistically correct.

$$RF = 0.003 - 0.0003\,Q + 0.002\,BH \qquad (6)$$

Table 3
Summary of p-value for the response surface modeling analysis for RF

Term	Full quadratic p-value[a]
Flow rate (Q)	0.000
pH	0.264
Bed height (BH)	0.003
$Q \times Q$	0.003
pH $\times$ pH	0.129
BH $\times$ BH	0.038
$Q \times$ pH	0.043
$Q \times$ BH	0.003
pH $\times$ BH	0.003
R^2 value, %; LOFT value	91.4; 0.241

[a]0.01–0.04: highly significant; 0.05–0.1: significant; 0.1–0.2: less significant; <0.2: insignificant.

Table 4
Value of the Bohart–Adams model parameters

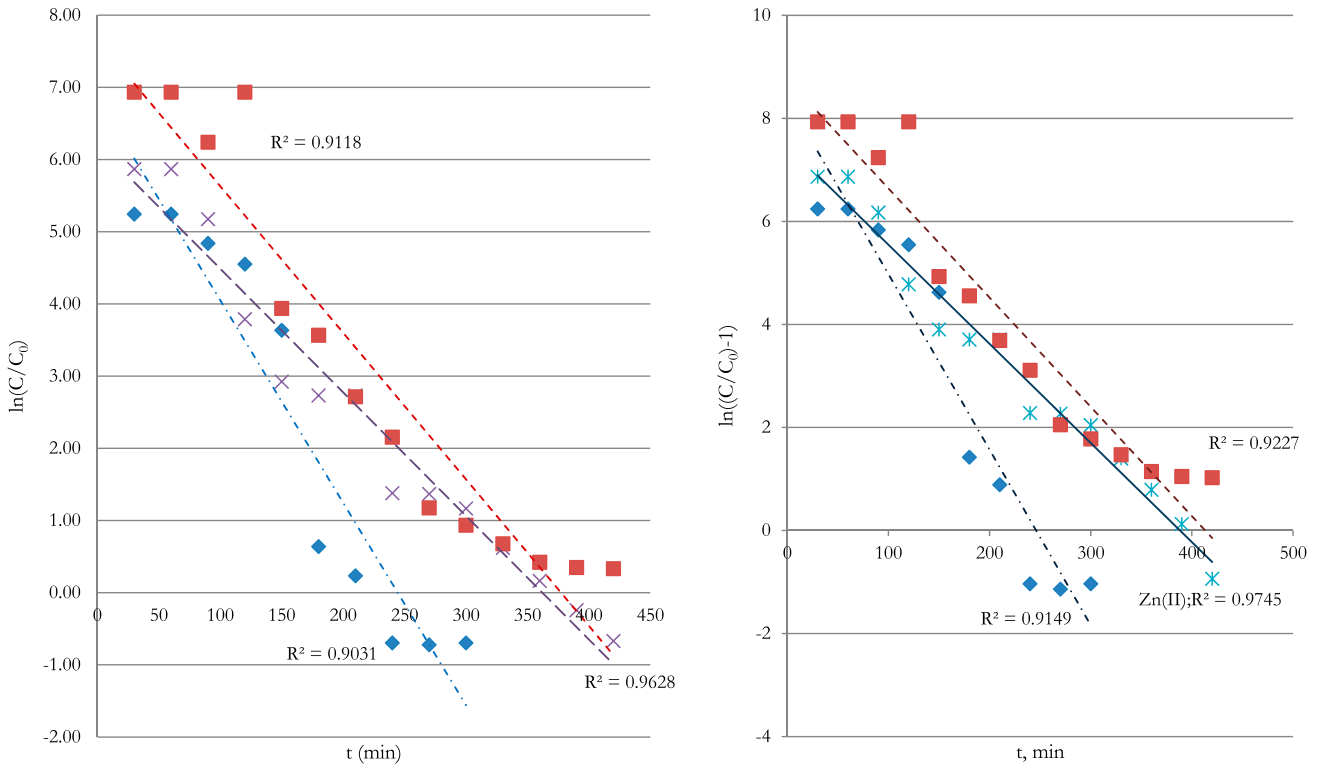| Parameter | Type of metals | | |
	Ni(II)	Zn(II)	Pb(II)
Q (cm^3 min^{-1})	12.0	15.2	20.0
Z (cm)	4.0	4.0	4.0
u (cm min^{-1})	3.8	4.8	6.4
C_o (mg cm^{-3})	0.001	0.0009	0.002
k_{BA} (mg min cm^{-3})	0.19	0.12	0.06
N_o (mg cm^{-3})	34.3	62.0	204.3
t_{br} (min)	150	150	210
R^2	0.90	0.96	0.91

Fig. 4. Linear plot of (a) Bohart–Adam model and (b) Thomas model with experimental data for different metal ions.
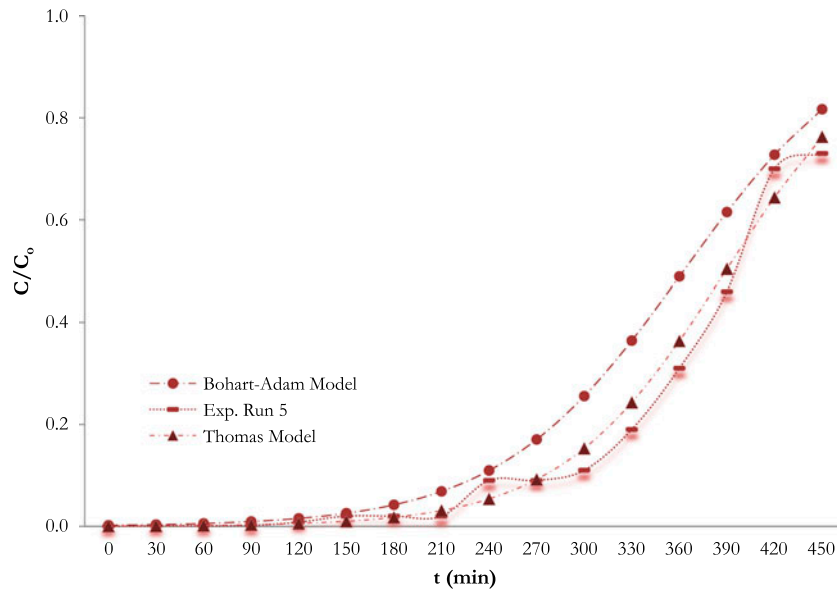

Fig. 5. Comparison of the experimental and theoretical breakthrough curves obtained at different flow rates and BHs for Bohart–Adam and Thomas Model for metal removal by the cation-exchange resin for experimental run 5 (Zn(II)).

Fig. 3 shows the 3D plot presenting the relationship between RF, flow rate, and BH, which illustrates the response surface obtained for Eq. (6). A very high efficiency of metal removal was obtained for all experiments (average 97.5%). The average efficiency of resin utilization (ε_f) varied in the range 40–95% for all
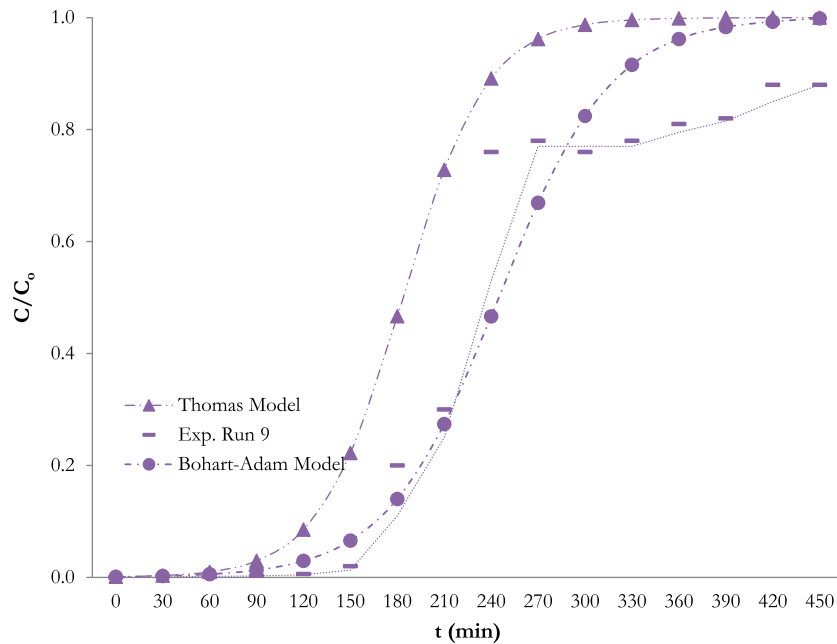
Fig. 6. Comparison of the experimental and theoretical breakthrough curves obtained at different flow rates and BHs for Bohart–Adam and Thomas Model for metal removal by the cation-exchange resin for experimental run 9 (Ni(II)).
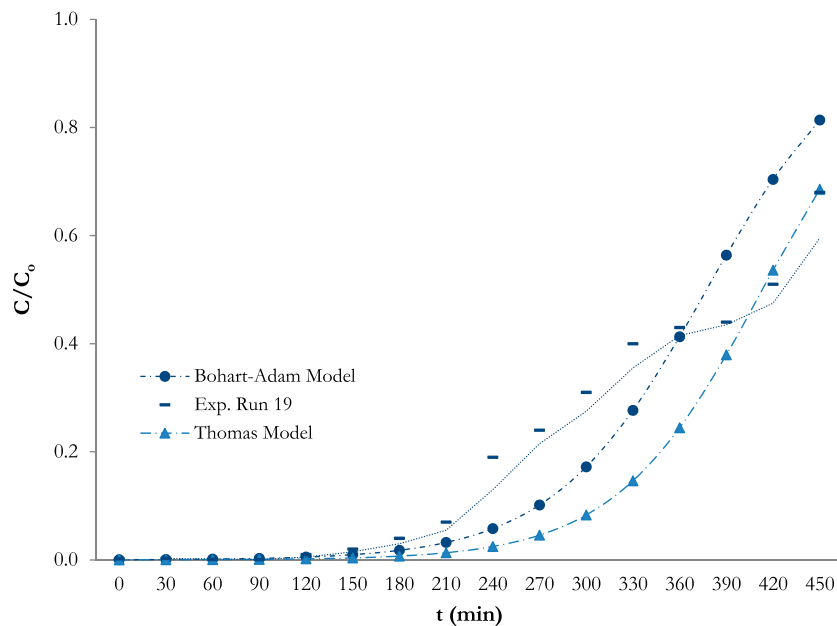

Fig. 7. Comparison of the experimental and theoretical breakthrough curves obtained at different flow rates and BHs for Bohart–Adam and Thomas Model for metal removal by the cation-exchange resin for experimental run 19 (Pb(II)).

metals. This shows that the potential capacity of the resin bed was utilized efficiently. These results also indicate that a decrease in the solution flow rate increases the efficiency of resin utilization.

3.3. Bohart–Adams model

The calculation of the theoretical breakthrough curves and the determination of the parameters K_{BA} and N_o for the solute of interest are listed in Table 4.

Table 5
Value of the Thomas model parameters

Parameter	Type of metals		
	Ni(II)	Zn(II)	Pb(II)
Q (mL min^{-1})	12.0	15.2	20.0
q_t (mg mg^{-1})	21.2	31.2	99.6
C_o (mg L^{-1})	0.001	0.0009	0.002
K_{TH} (mL mg min^{-1})	0.11	0.07	0.04
V (mL)	2,880	4,104	4,800
R^2	0.91	0.97	0.92

The approach involves a plot of $\ln[(C/C_o) - 1]$ vs. time according to Eq. (5) [20,21]. The Bohart–Adams model is applied to investigate the breakthrough behavior of metal (Ni(II), Zn(II), and Pb(II)) removal by the ion-exchange resin. The values of the kinetic constant and the maximum amount of metal exchange are determined from the $\ln(C/C_o)$ vs. t plots at different BHs and different flow rates with higher value of R^2 for each metals. These values are then used to determine the breakthrough curve.

From Table 4, it can be seen that the higher molecular weight of the metals resulted in higher exchange capacities (N_o). The values of the exchange capacities (N_o) were influenced by the changes in flow rates. The constant value of Bohart–Adam model increased by decreasing the flow rate. It is to be noted that the value of R^2 for Ni(II), Zn(II), and Pb(II) ions is 0.90, 0.96, and 0.91, respectively.

Bohart–Adams model is one of the simplest models for the breakthrough curve representation. The main assumption of this model is that the intraparticle diffusion and external resistance for mass transfer are negligible. The kinetics of adsorption was controlled by chemical reaction on the surface between the resins and the metal ions [32]. The consideration in this model is the adsorption as a reversible second-order reaction [33]. The theoretical curves are compared with the corresponding experimental data as shown in Figs. 5–7 for the removal of Zn(II), Ni(II), and Pb(II), respectively. It is shown that the experimental breakthrough curves are very closely related to those predicted by this model at the initial study. However, the model predicted curves and the corresponding experimental data did not perfectly match in the second part of the breakthrough curve. The possible explanation of this deviation may be due to the hydrodynamic phenomena, such as axial dispersion and the velocity gradients onto the column. Similar observation was reported upon applying Thomas and Bohart–Adams models for representing the removal of copper(II) ions

with biosorption by *Sargassum* sp. biomass in a fixed-bed column at 30°C and pH 3.5 [33].

In these three figures (Figs. 5–7), it was seen that the removal ratio (C/C_o) is less than 1.0. This may be due to the different affinity potential of metal ions into the resin. As the sorption proceeds, these metal ions (Ni(II), Zn(II), and Pb(II)) are competing against each other. In this ion-exchange process, it is seen that the presence of these three metal ions suppressed each other's uptake due to affinity towards the exchanging sites in Dowex 50W resins [34].

3.4. Thomas model

A theoretical model known as Thomas model was further applied to investigate the breakthrough behavior of the metals adsorption. The constants Thomas rate coefficients (K_{TH}) and maximum adsorption capacity (q_t) were calculated from the slope and intercepts of the plot between $\ln(C_o/C_t - 1)$ vs. t (Fig. 4(b)). The calculated values of K_{TH} and q_t along the regression coefficients are presented in Table 5. From Table 5, it can be observed that as the flow rate increased, the Thomas rates constant (K_{TH}) decreased, while the adsorption capacity (q_t) increased in series: Pb(II) > Zn(II) > Ni(II). Similar trends with Bohart–Adam model, the results also show that the higher the molecular weight of the metals, the higher the adsorption capacities (q_t). This observation was similar with Shahbazi et al. [10] which reported a removal of Pb(II), Cu(II), and Cd(II) by functionalized SBA-15 mesoporous silica by melamine-based dendrimer amines in batch and fixed-bed column. However, the q_t value increased and so is the Thomas rate constant for these three types of metal ions. Chowdhury and Saha [35] also made similar remarks for the adsorption of malachite green by modified rice husk in a fixed-bed column. It is to be noted that the relatively high R^2 (0.91, 0.97, and 0.92) of Ni(II), Zn(II), and Pb(II) ions, respectively. Therefore, this model provides a good fit to the experimental data compared with the Bohart–Adam model.

4. Conclusions

Experiments were conducted to study the breakthrough curves of Ni(II), Zn(II), and Pb(II) ions from aqueous solution using cation-exchange resins. The effects of the flow rate, pH, and BH on the RF of the column were considered for the determination of ion-exchange efficiency. The efficiency of solute removal was between 96 and 99%, and the values obtained for the efficiency of resin utilization were, in most cases, above 40%. The obtained results indicated that both

the breakthrough and saturation times increases at lower value of flow rates and higher resin BHs. This is because at a lower flow rate and higher BH, longer contact time is achieved, with a greater number of available binding sites, and the interaction between the metal and the resin is stronger. The exchange capacities (N_o, mg cm^{-3}) and adsorption capacities (q_t) increased in the sequence of Ni(II) < Zn(II) < Pb(II). The response surface analysis and the application of both models (Bohart–Adam and Thomas) gave good approximations of the observed experimental behavior. The Thomas model was found to be more appropriate model for describing the column adsorption data of these metal ions by Dowex 50W.

Acknowledgment

Nomenclature

C	—	effluent concentration (mg L^{-1})
C_o	—	inlet metal ion solutions (mg L^{-1})
t_{br}	—	breakthrough time
t_{end}	—	saturation time
ε_r	—	efficiency of solute removal
ε_f	—	efficiency of resin utilization
Q	—	volumetric flow rate (mL min^{-1})
K_{BA}	—	rate coefficient (cm^3 mg^{-1} min^{-1})
N_o	—	exchange capacity (mg cm^{-3})
Z	—	bed height (cm)
U_o	—	linear velocity (cm min^{-1}
t	—	time (min)
K_{TH}	—	rate coefficient (cm^3 mg^{-1} min^{-1})
$q_T m$	—	

References

[1] R. Petrus, J. Warchoł, Ion exchange equilibria between clinoptilolite and aqueous solutions of Na$^+$/Cu^{2+}, Na$^+$/Cd^{2+} and Na$^+$/Pb^{2+}, Microporous Mesoporous Mater. 61(1–3) (2003) 137–146.

[2] Department of Environment, Ministry of Science, Technology and Environment, Environmental Quality Report, Department of Environment, Malaysian Ministry of Science, Technology and Environment, Kuala Lumpur, 1997.

[3] O. Abdelwahab, N.K. Amin, E-S.Z. El-Ashtoukhy, Removal of zinc ions from aqueous solution using a cation exchange resin, Chem. Eng. Res. Des. 91 (2013) 165–173.

[4] N.H. Shaidan, U. Eldemerdash, S. Awad, Removal of Ni(II) ions from aqueous solutions using fixed bed ion exchange column technique, J. Taiwan Inst. Chem. Eng. 43 (2012) 40–45.

[5] J. Cruz-Olivares, C. Pérez-Alonso, C. Barrera-Díaz, F. Ureña-Nuñez, M.C. Chaparro-Mercado, Modeling of lead(II) biosorption by residue of allspice in a fixed bed column, Chem. Eng. J. 228 (2013) 21–27.

[6] B. Salamatinia, A.H. Kamaruddin, A.Z. Abdullah, Modeling of the continuous copper and zinc removal by sorption onto sodium hydroxide-modified oil palm frond in a fixed-bed column, Chem. Eng. J. 145 (2008) 259–266.

[7] R. Sharma, B. Singh, Removal of Ni(II) ions from aqueous solutions using modified rice straw in a fixed bed column, Bioresour. Technol. 146 (2013) 519–524.

[8] S. Mohan, G. Sreelakshmi, Fixed bed column study for heavy metal removal using phosphate treated rice husk, J. Hazard. Mater. 153 (2008) 75–82.

[9] A.P. Lim, A.Z. Aris, Continuous fixed-bed column study and adsorption modeling: Removal of cadmium (II) and lead(II) ions in aqueous solution by dead calcareous skeletons, Biochem. Eng. J. 87 (2014) 50–61.

[10] A. Shahbazi, H. Younesi, A. Badiei, Functionalized SBA-15 mesoporous silica by melamine-based dendrimer amines for adsorptive characteristics of Pb(II), Cu(II) and Cd(II) heavy metal ions in batch and fixed bed column, Chem. Eng. J. 168 (2011) 505–518.

[11] H. Kalavathy, B. Karthik, L.R. Miranda, Removal and recovery of Ni and Zn from aqueous solution using activated carbon from *Hevea brasiliensis*: Batch and column studies, Colloids Surf., B 78 (2010) 291–302.

[12] T.A. Saleh, V.K. Gupta, A.A. Al-Saadi, Adsorption of lead ions from aqueous solution using porous carbon derived from rubber tires: Experimental and computational study, J. Colloid Interface Sci. 396 (2013) 264–269.

[13] E. Pehlivan, T. Altun, The study of various parameters affecting the ion exchange of Cu^{2+}, Zn^{2+}, Ni^{2+}, Cd^{2+}, and Pb^{2+} from aqueous solution on Dowex 50W synthetic resin, J. Hazard. Mater. 134(1–3) (2006) 149–156.

[14] D. Liu, Z. Li, Y. Zhu, Z. Li, R. Kumar, Recycled chitosan nanofibril as an effective Cu(II), Pb(II) and Cd (II) ionic chelating agent: Adsorption and desorption performance, Carbohydr. Polym. 111 (2014) 469–476.

[15] A.H. Elshazly, A.H. Konsowa, Removal of nickel ions from wastewater using a cation-exchange resin in a batch-stirred tank reactor, Desalination 158 (2003) 189–193.

[16] E. Pehlivan, T. Altun, Ion-exchange of Pb^{2+}, Cu^{2+}, Zn^{2+}, Cd$^{2+,}$ and Ni^{2+} ions from aqueous solution by Lewatit CNP 80, J. Hazard. Mater. 140 (2007) 299–307.

[17] M. Hafizi, H. Abolghasemi, M. Moradi, S.A. Milani, Strontium adsorption from sulfuric acid solution by Dowex 50W-X resins, Chin. J. Chem. Eng. 19(2) (2011) 267–272.

[18] B. Alyüz, S. Veli, Kinetics and equilibrium studies for the removal of nickel and zinc from aqueous solutions by ion exchange resins, J. Hazard. Mater. 167(1–3) (2009) 482–488.

[19] E.I. Unuabonah, B.I. Olu-Owolabi, E.I. Fasuyi, K.O. Adebowale, Modeling of fixed-bed column studies for the adsorption of cadmium onto novel polymer–clay composite adsorbent, J. Hazard. Mater. 179 (2010) 415–423.

[20] O. Hamdaoui, Removal of copper(II) from aqueous phase by Purolite C100-MB cation exchange resin in fixed bed columns: Modeling, J. Hazard. Mater. 161 (2009) 737–746.

[21] K.H. Chu, Fixed bed sorption: Setting the record straight on the Bohart–Adams and Thomas models, J. Hazard. Mater. 177 (2010) 1006–1012.

[22] M. Kragović, A. Daković, Ž. Sekulić, M. Trgo, M. Ugrina, J. Perić, G.D. Gatta, Removal of lead from aqueous solutions by using the natural and Fe(III)-modified zeolite, Appl. Surf. Sci. 258 (2012) 3667–3673.

[23] E.C. Cren, L.C. Cardozo Filho, E.A. Silva, A.J.A. Meirelles, Breakthrough curves for oleic acid removal from ethanolic solutions using a strong anion exchange resin, Sep. Purif. Technol. 69 (2009) 1–6.

[24] C.P. Dwivedi, J.N. Sahu, C.R. Mohanty, B. Mohan, B.C. Meikap, Column performance of granular activated carbon packed bed for Pb(II) removal, J. Hazard. Mater. 156 (2008) 596–603.

[25] V.C. Taty-Costodes, H. Fauduet, C. Porte, Y.-S. Ho, Removal of lead(II) ions from synthetic and real effluents using immobilized *Pinus sylvestris* sawdust: Adsorption on a fixed-bed column, J. Hazard. Mater. 123 (2005) 135–144.

[26] R. Gandhimathi, S.T. Ramesh, P.V. Nidheesh, B. Nagendra, K.S. Bharathi, Breakthrough data analysis of adsorption of Cd(II) on coir pith column, EJEAFChe. 10(7) (2011) 2487–2505.

[27] P.N. Palanisamy, P. Sivakumar, Kinetic and isotherm studies of the adsorption of Acid Blue 92 using a low-cost non-conventional activated carbon, Desalination 249 (2009) 388–397.

[28] A.S. Darwish, T.M. Zewail, N.S. Yousef, Y.A. El-Tawail, Investigation of the performance of a batch air spouting bed in conducting ion exchange reactions involving heavy metal removal, J. Taiwan Inst. Chem. Eng. 47 (2015) 171–176.

[29] F. Gode, E. Pehlivan, Removal of chromium(III) from aqueous solutions using Lewatit S 100: The effect of pH, time, metal concentration and temperature, J. Hazard. Mater. 136 (2006) 330–337.

[30] M. Mahmoud Nasef, H. Saidi, Z. Ujang, K.Z. Mohd Dahlan, Removal of metal ions from aqueous solutions using crosslinked polyethylene-GTMFJ-polystyrene sulfonic acid adsorbent prepared by radiation grafting, J. Chil. Chem. Soc. 55(4) (2010) 421–427.

[31] M.M. Nasef, Z. Ujang, Introduction to ion-exchange processes, in: I. Sediqi, M. Luqman (Eds.), Ion-Exchange Technology: Theory, Materials and Applications, Springer Science, New York, NY, 2012, pp. 1–39.

[32] P. Lodeiro, B. Cordero, J.L. Herrero, M.E. Sastre de Vieene, The use of protonated *Sargassum muticum* as biosorbent for cadmium removal in a fixed-bed column, J. Hazard Mater. B137 (2005) 244–253.

[33] C.E. Borba, E. Silva, M.R. Fagundes-Klen, A.D. Kroumov, R. Guirardello, Prediction of the copper(II) ions dynamic removal from a medium by using mathematical models with analytical solution, J. Hazard. Mater. 152 (2008) 366–372.

[34] M.A.S.D. Barros, P.A. Arroyo, E.A. Silva, in: H. Nakajima (Ed.), Mass Transfer-Advances in Sustainable Energy and Environment Oriented Numerical Modeling, INTECH, Rijeka, Croatia, 2013, pp. 361–386.

[35] S. Chowdhury, P.D. Saha, Adsorption of malachite green from aqueous solution by NaOH-modified rice husk: Fixed-bed column studies, Environ. Prog. Sustainable Energy 32(3) (2013) 633–639.